Eur. Phys. J. B **37**, 311–320 (2004)
DOI: 10.1140/epjb/e2004-00061-9

THE EUROPEAN PHYSICAL JOURNAL B

Ab initio study of the Fe intra- and inter-layer magnetic order in Fe/Ir(001) superlattices

D. Stoeffler[a]

IPCMS-Gemm (UMR 7504 du CNRS), 23 rue du Loess, 67034 Strasbourg, France

Received 7 July 2003 / Received in final form 1st December 2003
Published online 2 April 2004 –

Abstract. An ab initio study of the magnetic behaviour of strained Fe/Ir(001) superlattices is presented using the first principle Augmented Spherical Wave method. First, the intralayer magnetic order of the Fe layers is examined as a function of their tetragonal distortion induced by the superlattice structure. It is shown that (i) an antiferromagnetic order can not occur, (ii) a ferrimagnetic phase, characterized by interfacial Fe magnetic moments opposite to the others, is allowed in a large domain of distortions, (iii) first order transitions toward the ferromagnetic (non magnetic) phase occur when the tetragonal distortion is (respectively) reduced at constant atomic volume (in plane lattice parameter) and (iv) when the Fe thickness increases, the ferromagnetic/ferrimagnetic transition is shifted to higher tetragonal distortions. Second, the interlayer magnetic couplings are determined in $Fe_5Ir_n(001)$ superlattices with the Fe layer in the relaxed body centered cubic structure with $n = 1$ to 11 monolayers. It is shown that the coupling energy decreases surprisingly slowly (like $1/n$) with increasing n with a period of approximately 3.2 monolayers, which corresponds nicely to the period of the Ir induced polarisation. Finally, these results are discussed in relation with experimental studies.

PACS. 75.30.Et Exchange and superexchange interactions – 75.70.-i Magnetic properties of thin films, surfaces, and interfaces – 75.70.Cn Magnetic properties of interfaces (multilayers, superlattices, heterostructures)

1 Introduction

Metallic multilayers have been intensively studied during this two last decades and remain up to now for their promising technological applications and their fundamental aspects in the physics of reduced dimension systems. Usually, most of studies are devoted to the interlayer exchange couplings, the giant magnetoresistance and, to the quantum wells properties. However, multilayered systems can also be used for exploring the magnetic properties of strained thin films as illustrated by this paper. From a fundamental point of view, it is well known that the magnetic properties of transition metals are highly sensitive to small structural changes, to the thickness of the magnetic layer and to the boundary conditions at the interfaces with the spacer layer. Building multilayers is one of the most powerful tool to explore this sensitivity. Indeed, when an epitaxial growth is obtained (usually for small thickness), the thin films are constrained and adopt an out of equilibrium structure: by varying the relative thickness of the magnetic and the non magnetic layer, the stress can be a priori controlled and a wide range of structures can be explored. Of course, in order to study the relation between distortion and magnetic properties, an extremely high structural characterisation is needed which is not always the case. Fe/Ir (001) superlattices studied extensively by the University of Nancy solid state group [1–14] is a system for which both accurate structural and magnetic experimental studies are available and their results offer a good opportunity to be compared to the simulated properties. Surprisingly, nearly no electronic structure calculations of these superlattices have been reported in the literature.

By combining structural and magnetic studies, it has been shown the important role played by the structure on the magnetic properties of Fe/Ir(001) multilayers. Let us summarize the main results concerning the magnetic behaviour. First, the Fe layer presents a strong tetragonal distortion ($c/a = 1.25$) for small thickness and relaxes to the bulk body centred cubic (BCC) structure for large thickness. The thickness increase induces a transition from a non-magnetic state toward a poorly magnetized one in the tetragonal phase and toward a ferromagnetic state when the BCC phase is recovered [7]. Moreover, in the tetragonal phase, even if the central Fe atoms carry a high local magnetic moment, the average magnetisation in the Fe layer remains small [9] and corresponds to two magnetically dead Fe atomic layers [8]. Local investigations with Mössbauer spectroscopy have confirmed that,

[a] e-mail: daniel.stoeffler@ipcms.u-strasbg.fr

Table 1. Values of the c by a ratio of the body centred tetragonal (BCT) structure obtained for the values of the (001) in plane lattice constant a and the Wigner-Seitz radius R_{Fe} corresponding to the nodes of the (α, ρ) grid used in this work. Note that the c/a ratio is nearly constant along oblique lines.

	$\alpha = -1\%$ $a = 4.9633$ a.u.	$\alpha = -0.5\%$ $a = 4.9884$ a.u.	$\alpha = 0\%$ $a = 5.0134$ a.u.	$\alpha = 0.5\%$ $a = 5.0385$ a.u.
$\rho = 0.5\%$ $R_{\mathrm{Fe}} = 2.6847$ a.u.	1.3258	1.3059	1.2864	1.2673
$\rho = 0\%$ $R_{\mathrm{Fe}} = 2.6713$ a.u.	1.3061	1.2865	1.2673	1.2485
$\rho = -0.5\%$ $R_{\mathrm{Fe}} = 2.6580$ a.u.	1.2866	1.2673	1.2484	1.2299
$\rho = -1\%$ $R_{\mathrm{Fe}} = 2.6446$ a.u.	1.2673	1.2483	1.2297	1.2114
$\rho = -1.5\%$ $R_{\mathrm{Fe}} = 2.6313$ a.u.	1.2482	1.2295	1.2112	1.1932

for 4 Fe atomic layers, the two central Fe atomic layers bear a noticeable magnetic moment and that the two interfacial Fe atomic layers are nearly non-magnetic [12]. This suggests the occurrence of a complex magnetic order in the Fe layers resulting from the tetragonal distortion with magnetic moments cancelling each other's. Finally, an interlayer magnetic coupling has been obtained in the BCC phase oscillating as a function of the Ir thickness with a period of 3.5 Å [5].

In this paper, we present a theoretical study of the magnetic behaviour of $\mathrm{Fe}_m\mathrm{Ir}_n(001)$ superlattices using the ab initio Augmented Spherical Waves (ASW) method [15]. First, we study the role of the tetragonal distortion by determining the magnetic phase diagram for $\mathrm{Fe_3Ir_5}$, $\mathrm{Fe_4Ir_4}$ and $\mathrm{Fe_5Ir_5}$ superlattices. Second, we determine the interlayer magnetic couplings in $\mathrm{Fe_5\ Ir}_n(001)$ superlattices when the Fe layer is relaxed in the BCC structure with $n = 1$ to 11 monolayers.

2 Methodology

For determining the magnetic properties of small superlattices, we use the first principle Augmented Spherical Wave (ASW) method allowing to obtain in a very accurate way the electronic structure of these metallic systems within the Local Spin Density Approximation (LSDA) formalism for treating exchange and correlation of a many electron system. This method has been used successfully by several authors for studying the relation between the structure, the layers thickness, the interfacial mixing and the magnetism [16–19]. It represents a good compromise between computer time and accuracy. The Atomic Sphere Approximation (ASA) is also used and limits the application of such a method for studying the relaxation in order to determine the structural ground state. However, the method is efficient for studying the magnetic ground state for a given structure, which is exactly the case of this work.

The role played by the tetragonal distortion of the Fe layer is studied by varying the in plane parameter a of the Fe body centred tetragonal (BCT) cell and the atomic volume radius R_{Fe} of the Fe atoms. Because the ASA is used, the ratio c/a of the perpendicular to plane parameter c and the in plane parameter a is equal to $(8\pi/3)(R_{\mathrm{Fe}}/a)^3$. Thus the two dimensional magnetic phase diagram is obtained by determining the most stable magnetic state for all (a, R_{Fe}) values. However, because the total energy calculation of a given magnetic state needs a large among of computer time, it is not possible to vary a and R_{Fe} over a to large range of values. This is why we determine the total energy $E_{tot}(\mathrm{MS})$ of a given magnetic state MS for a discrete set of (a, R_{Fe}) values and we interpolate the surface $E_{tot}(a, R_{\mathrm{Fe}}; \mathrm{MS})$ by a third order polynomial function $P_{\mathrm{MS}}(a,\ R_{\mathrm{Fe}})$. We have then the possibility to compare the interpolated total energies for various MS and to determine accurately the stability domain of each MS. Finally, for each calculation, the number of K points used in the irreducible part of the Brillouin Zone is increased up to the convergence of the total energy which is usually the case with approximately 500 K points.

3 Magnetic phase diagrams in $\mathrm{Fe_mIr_n}$ superlattices

In this section, we have to determine the most stable magnetic state in Fe layers for a given set of crystalline structures characterized by the pair of (a, R_{Fe}) values. It is more convenient to work with relative values for the tetragonal distortion than to used directly the in plane parameter a of the Fe body centred tetragonal (BCT) cell and the atomic volume radius R_{Fe} of the Fe atoms. This is why we introduce the α and ρ variations of these two values ($a = (1+\alpha)a_{ref}$, $R_{\mathrm{Fe}} = (1+\rho)R_{\mathrm{Fe},ref}$) relative to the reference $(a_{ref}, R_{\mathrm{Fe},ref}) = (5.01344$ a.u., 2.67132 a.u.) which correspond approximately to the average experimental values. Table 1 gives the values of the sets (α, ρ) used in this work with the corresponding c/a ratio of the tetragonal distortion. With this set, the c/a ratio is varied from 1.19 up to 1.32. Similarly, the atomic volume radius of the Ir atoms corresponds approximately to the average experimental values and is chosen equal to 2.8072 a.u.: it is assumed to not be affected by variations of α and ρ and to not vary for all calculations. This assumption is made

Table 2. Values of the magnetic moments M_{FM} and M_{AFM} (in μ_B) obtained for the bulk BCT structure for all nodes of the (α, ρ) grid for the ferromagnetic (FM) and the antiferromagnetic (AFM) orders. The second line gives the total energy differences $\Delta E_{\mathrm{AFM-FM}}$ and $\Delta E_{\mathrm{NM-FM}}$ (in meV per atom) between the AFM and the FM solutions and between the non magnetic (NM) and the FM ones.

$M_{\mathrm{FM}}/M_{\mathrm{AFM}}$	$\alpha = -1\%$	$\alpha = -0.5\%$	$\alpha = 0\%$	$\alpha = 0.5\%$
$\Delta E_{\mathrm{AFM-FM}}/\Delta E_{\mathrm{NM-FM}}$	$a = 4.9633$ a.u.	$a = 4.9884$ a.u.	$a = 5.0134$ a.u.	$a = 5.0385$ a.u.
$\rho = 0.5\%$	2.49 / 1.57	2.44 / 1.22	2.39 / 0.98	2.34 / 0.76
$R_{\mathrm{Fe}} = 2.6847$ a.u.	10.5 / 40.4	9.7 / 27.0	10.4 / 19.1	12.3 / 15.8
$\rho = 0\%$	2.42 / 1.25	2.36 / 0.98	2.32 / 0.76	2.29 / 0.48
$R_{\mathrm{Fe}} = 2.6713$ a.u.	9.0 / 25.7	9.8 / 18.2	12.2 / 15.5	14.8 / 15.9
$\rho = -0.5\%$	2.33 / 0.98	2.29 / 0.76	2.26 / 0.49	2.25 / 0.02
$R_{\mathrm{Fe}} = 2.6580$ a.u.	8.9 / 17.4	11.7 / 14.5	15.1 / 15.9	18.6 / 18.6
$\rho = -1\%$	2.26 / 0.76	2.24 / 0.49	2.22 / 0.01	2.21 / 0.00
$R_{\mathrm{Fe}} = 2.6446$ a.u.	10.5 / 13.7	14.5 / 15.0	18.9 / 18.9	24.5 / 24.5
$\rho = -1.5\%$	2.22 / 0.48	2.20 / 0.05	2.19 / 0.00	2.18 / 0.00
$R_{\mathrm{Fe}} = 2.6313$ a.u.	13.4 / 13.9	18.0 / 18.1	24.3 / 24.3	32.5 / 32.5

in order to not vary too much parameters at the same time (to not have to work in a 3 dimensionnal space (a, R_{Fe}, R_{Ir})) and corresponds to a good approximation of the experimental behaviour for such small variation of a. In this work, the aim is to focuss on the competition between the "intrinsic" magnetic ordering of a BCT Fe thin layer (which should behave like the bulk BCC Fe one for large thickness) and the ordering induced at the boundaries by the Fe-Ir hybridization. An additional variation of the Ir atomic volume acts certainly less on this competition than the distortion of the Fe structure itself and is considered as being a second order term. Finally, when a and the atomic volume radius R_i of all atoms are given, the distance between the ith and the $(i+1)$th planes is obtained from $d = (2\pi/3)(R_i^3 + R_{i+1}^3)/a^2$.

3.1 Bulk BCT Fe

Before studying thin Fe layers in Fe/Ir superlattices, it is interesting to investigate the magnetic behaviour of bulk BCT Fe for the same set of tetragonal distorted structures. It is well established that the Fe magnetic order undergoes a transition from ferromagnetic to antiferromagnetic when the structure changes from body centred cubic (BCC) to face centred cubic (FCC). It has also been shown that the antiferromagnetic order presents a first order transition from a low towards a high magnetic moment state. It is essential for the understanding of our results to check if the range of c/a we are studying induces such behaviour or not.

Table 2 summarises the results we have obtained considering the relative stability of ferromagnetic (FM), antiferromagnetic (AFM) and non magnetic (NM) states for all BCT structures listed in Table 1. For the FM state, our calculations show that (i) it is the most stable one with a magnetic moment ranging from 2.18 to 2.49 μ_B for the extreme values of c/a, (ii) its magnetic moment is more sensitive to tetragonal distortions at constant atomic volume (ρ being constant and α varying) when the atomic volume is larger. For the AFM state, we found that (i) it appears with a second order transition from the NM to the AFM state for c/a values around 1.23 with a rapidly increasing magnetic moment reaching 1.57 μ_B for the highest c/a value, (ii) the energy difference with the FM state decreases when the tetragonal distortion increases as expected since the AFM state becomes the most stable one when the FCC structure (corresponding to $c/a = \sqrt{2}$) is reached [20]. It is interesting to note that the magnetic moments and the energy differences change only slightly along the diagonal of Table 2, which corresponds, nearly to variations at constant c/a values.

This study shows that the FM state is the bulk BCT Fe magnetic ground state for all structures considered and that the essential parameter is the c/a ratio.

3.2 Competing magnetic orders in thin Fe layers

As previously shown, around the bulk BCT structure for the experimental c/a ratio of 1.25 [7], the AFM solution coexists with the FM one (even if the second is most stable) in bulk BCT Fe. Consequently, when we consider thin Fe layers with increasing thickness, the number of possible magnetic configurations increases because all relative magnetic moments ordering can be a priori stabilised in the calculation even if we restrict our study to one atom in the in plane cell. For example, if a positive (negative) magnetic moment is represented by $\uparrow$ ($\downarrow$), with 3 Fe monolayers we can have 3 different magnetic configurations $\uparrow\uparrow\uparrow$, $\uparrow\uparrow\downarrow$ or $\uparrow\downarrow\uparrow$, with 4 Fe monolayers we can have $\uparrow\uparrow\uparrow\uparrow$, $\uparrow\uparrow\uparrow\downarrow$, $\uparrow\uparrow\downarrow\uparrow$, $\uparrow\uparrow\downarrow\downarrow$, $\uparrow\downarrow\downarrow\uparrow$ or $\uparrow\downarrow\uparrow\downarrow$, with 5 Fe monolayers we can have $\uparrow\uparrow\uparrow\uparrow\uparrow$, $\uparrow\uparrow\uparrow\uparrow\downarrow$, $\uparrow\uparrow\uparrow\downarrow\uparrow$, $\uparrow\uparrow\downarrow\uparrow\uparrow$,$\uparrow\uparrow\uparrow\downarrow\downarrow$, $\uparrow\uparrow\downarrow\downarrow\uparrow$, $\uparrow\uparrow\downarrow\uparrow\downarrow$, $\uparrow\downarrow\downarrow\downarrow\uparrow$ or $\uparrow\downarrow\uparrow\downarrow\uparrow$, ... Of course, we do not pretend to study systematically all these possible solutions. The aim of this work is more to exhibit stable non-FM configurations in order to show that situations with a reduced magnetisation due to compensating magnetic moments are possible solutions. This is why we restrict our study to the configurations given in Table 3: the ferromagnetic (FM) one for which all moments are parallel, the ferrimagnetic (FiM)

Table 3. Schematic representation of the magnetic orders considered in the Fe layers for the Fe_mIr_n superlattices considered in this work. Each arrow corresponds to the magnetic moment of an atomic plane.

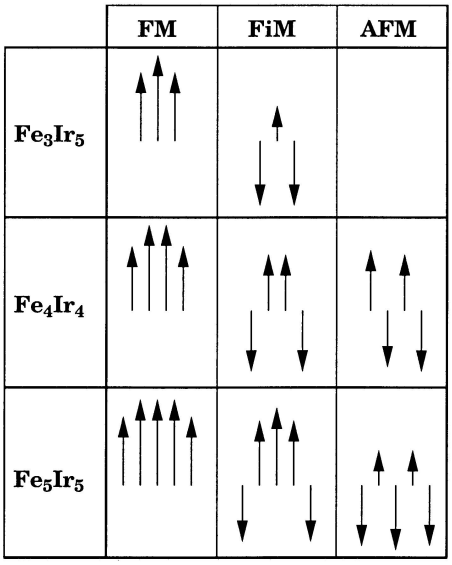

one for which the interfacial magnetic moments are opposite to the inner ones and the antiferromagnetic (AFM) one which corresponds to an antiferromagnetic order from monolayer to monolayer (for 3 Fe monolayers, the FiM and AFM cases are the same).

3.3 Electronic structure of Fe_mIr_n superlattices for $(\alpha, \rho) = (0, 0)$

Because most of the new features come from the interface, it is interesting to discuss the local densities of states (LDOS) in terms of interfacial Fe-Ir hybridisation. Figures 1, 2 and 3 show the LDOS for Fe_3Ir_5 superlattices with $\alpha = 0$ and $\rho = 0$ which are representative of the LDOS for other Fe or Ir thickness and other values of α and ρ.

For the NM case (Fig. 1), we see that the LDOS are very similar for all Fe atoms – on the central (C) atomic plane or on the interfacial (I) one – and very similar for all Ir atoms – on the interfacial (I) atomic plane, the next one (I+1) and the central (C) one. This shows that the Fe-Ir interfacial hybridisation induces only small modifications in the electronic structure of thin Fe or Ir layers. The main feature coming from the Fe-Ir hybridisation is the small peak in the Fe LDOS around −5.7 eV – surprisingly more pronounced on the C site than on the I one – which corresponds to a large peak in the Ir interfacial LDOS. The other characteristics of the LDOS are very similar to the bulk BCT one which for the Fe atoms looks more like a face centred cubic (FCC) LDOS than a body centred cubic (BCC) one showing than for the values of c/a considered in this work, the Fe thin layer has an electronic structure similar to the one of a FCC layer.

For the FM case (Fig. 2), the main features mentioned previously for the NM case remain valid. The most

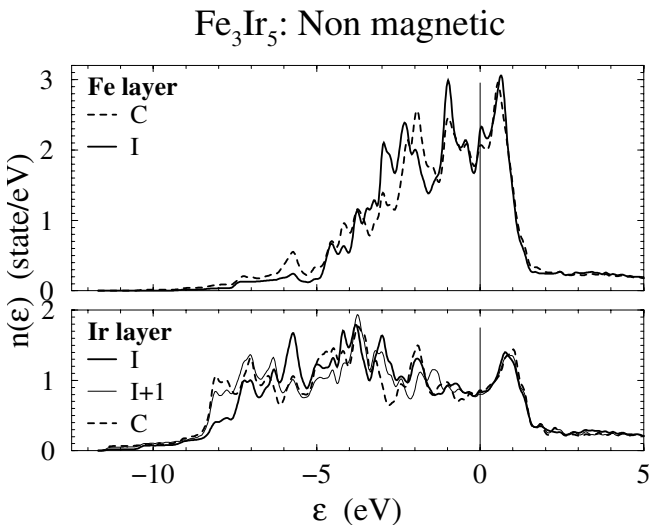

Fig. 1. Local densities of states for all non-equivalent sites (C for central, I for interfacial and I+1 for the atomic plane between C and I in the Ir layer) for Fe_3Ir_5 superlattices for the non-magnetic situation.

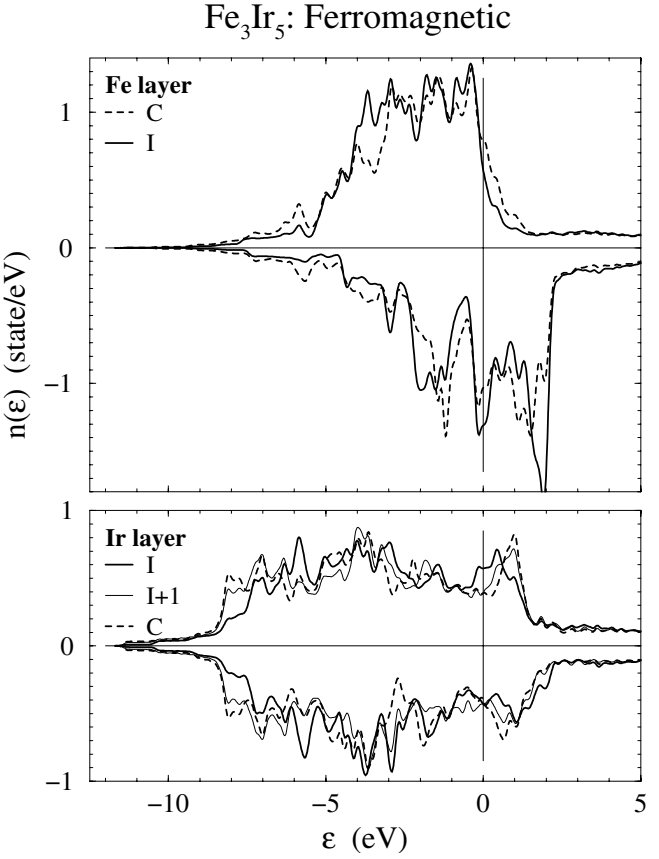

Fig. 2. Local densities of states for all non-equivalent sites (C for central, I for interfacial and I+1 for the atomic plane between C and I in the Ir layer) for Fe_3Ir_5 superlattices for the ferromagnetic situation. Positive values correspond to the majority spin states and negative values to the minority spin states.

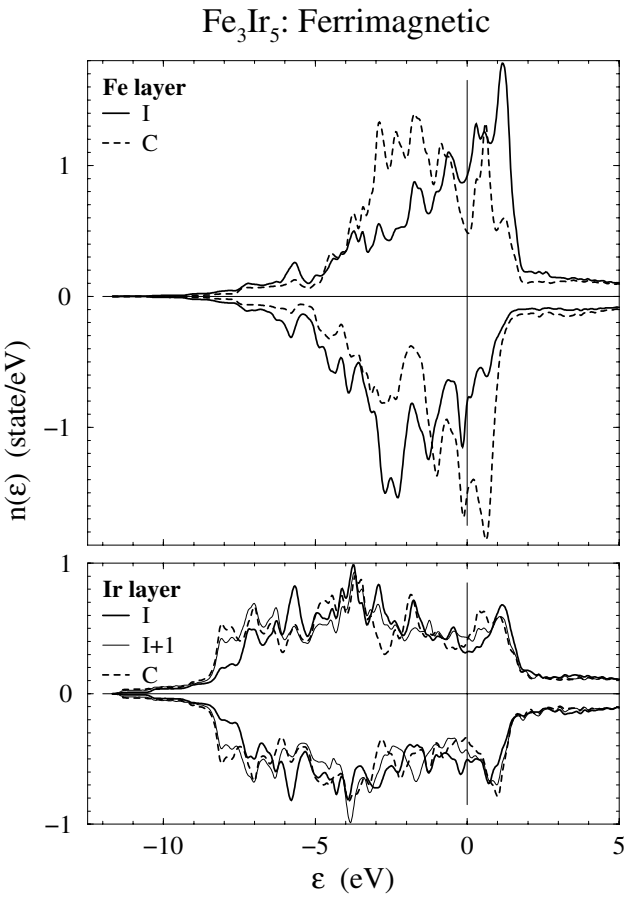

Fig. 3. Local densities of states for all non-equivalent sites (C for central, I for interfacial and I+1 for the atomic plane between C and I in the Ir layer) for Fe_3Ir_5 superlattices for the ferrimagnetic situation. Positive values correspond to the majority spin states and negative values to the minority spin states.

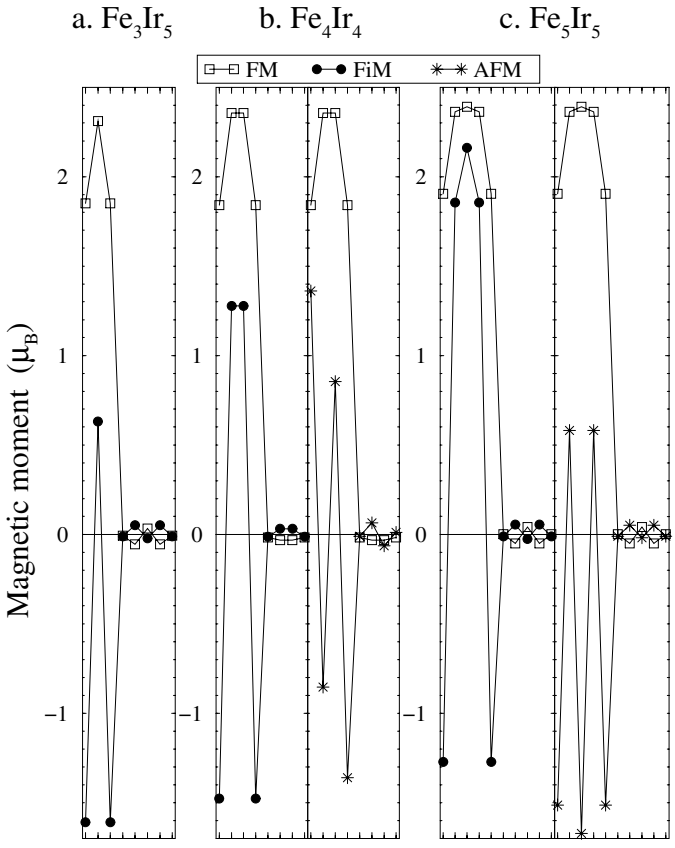

Fig. 4. Magnetic moments profiles for a) Fe_3Ir_5, b) Fe_4Ir_4 and c) Fe_5Ir_5 superlattices for the ferromagnetic (FM), ferrimagnetic (FiM) and antiferromagnetic (AFM) configurations of the Fe layers. The Fe sites carry the large magnetic moments.

significant changes can be seen on the majority spin LDOS – the minority spin one being very similar to the NM one – which presents less pronounced peaks as compared to the minority spin one or the NM LDOS. This is due to the fact that most of the majority spin states have been shifted below the Fermi level allowing a higher level of hybridisation because more states are available at this lower range of energy (between −5 and −2.5 eV) coming from the Ir layer. This shows that the Fe-Ir hybridisation, even if its remains small, is more pronounced for the majority spin states than for the minority ones.

For the FiM case (Fig. 3), we can expect that both majority and minority spin LDOS be affected because there are opposite magnetic moments in the Fe layer. This is effectively what we obtain: the majority spin LDOS on the C atomic layer and the minority spin LDOS on the I atomic layer are the most affected because they correspond to the spin direction aligned with the local magnetic moment and correspond to the states which are shifted below the Fermi level in the same way than all majority spin LDOS for the FM case. Moreover, because the C magnetic moments are opposite to the I ones, there is a much higher mixing between both spin states explaining why all Fe LDOS have the top of the d band nearly at the same energy whereas, for the FM case, the top of the minority spin d band is more than 2 eV higher than the top of the majority one. The Ir LDOS show no significant changes when compared with the NM and the FM ones.

To conclude this section, we have shown that the states corresponding to the spin direction aligned with the local magnetic moment are the most affected by the Fe-Ir hybridisation.

3.4 Magnetic moments profiles in Fe_mIr_n superlattices for $(\alpha, \rho) = (0, 0)$

The magnetic moments profile for the 3 superlattices and for the different Fe layer magnetic orders we consider are presented in Figure 4. The magnetic moments carried by the Ir atoms are found small (less than 0.1 μ_B) and particularly small at the interface with the Fe layer as a consequence of the weak Fe-Ir hybridisation discussed previously. The magnetic moments profiles in the Ir spacer present rapid oscillations (mainly visible for the 5 monolayer thick spacer) with a magnetic moment on the second

atomic plane (counted from the Fe/Ir interface) always opposite to the interfacial Fe one. The magnetic moments on the Fe sites are significantly affected by the various orders considered but present monotonic behaviour with increasing Fe layers thickness. For the FM case, the interfacial sites carry a reduced magnetic moment (around 1.9 μ_B), resulting from Fe-Ir hybridisation which enlarges the LDOS and weakens the ferromagnetism on the interfacial Fe site, whereas the inner sites carry a nearly bulk-like value (around 2.4 μ_B) showing that the interfacial perturbation is really short ranged. For the FiM case, the magnitude of the magnetic moments on the interfacial sites decreases (from -1.6 to -1.3 μ_B) whereas the moments on the inner sites increase (from around 0.6 to around 2 μ_B) with increasing Fe thickness. This seems to be an indication of a less tolerated magnetic anti-alignment of the inner sites as compared to the interfacial ones, the interfacial Fe moments being found larger than the ones for the corresponding bulk BCT AFM order as shown in Table 2. This is also supported by a rapid increase of the magnetic moment on the inner sites when a ferromagnetic environment is recovered as shown in Figure 4c. Even for the AFM case, where no ferromagnetic order between atomic planes is allowed, the magnetic moments are surprisingly enhanced as compared to the bulk BCT values. This shows that the interface with Ir favours antiparallel alignment between Fe magnetic moments.

3.5 Magnetic moments (α, ρ) maps

The comparison between the local magnetic moments on the non-equivalent Fe sites for the 3 superlattices considered in this section is displayed in Figures 5, 6 and 7 for respectively Fe_3Ir_5, Fe_4Ir_4 and Fe_5Ir_5. In Figure 5 is also reported the bulk BCT magnetic moments for all (α, ρ) values.

It can be clearly seen in Figure 5 that the magnetic response of a 3 monolayer thick Fe layer to structural variations is completely different from the bulk BCT one. Effectively, for the FM case, whatever the value of ρ is, the local magnetic moments in the thin layer increase when α increases contrary to the bulk BCT magnetic moment. Moreover, the magnetic moments in the thin layer vary more significantly over the range of α values than in the bulk BCT; these variations are more pronounced when ρ is smaller i.e. when the atomic volume is compressed. When the Fe layer thickness increases (Figs. 6 and 7), these variations become less pronounced due to a larger bulk-like contribution. However, even for Fe_5Ir_5 superlattices (Fig. 7) , the bulk BCT behaviour is not recovered. This confirms the enhanced sensitivity of the ferromagnetism in these thin Fe layers.

For the FiM case and for Fe_3Ir_5 superlattices, the situation is exactly the opposite to the FM case: the local magnetic moments vary more slowly when α varies for the thin Fe layers than for the bulk BCT situation. More surprising are the nearly constant values of the magnetic moments in the thin layer for a given ρ (-1.5% to -0.5%) with increasing α values whereas they vanish in the bulk

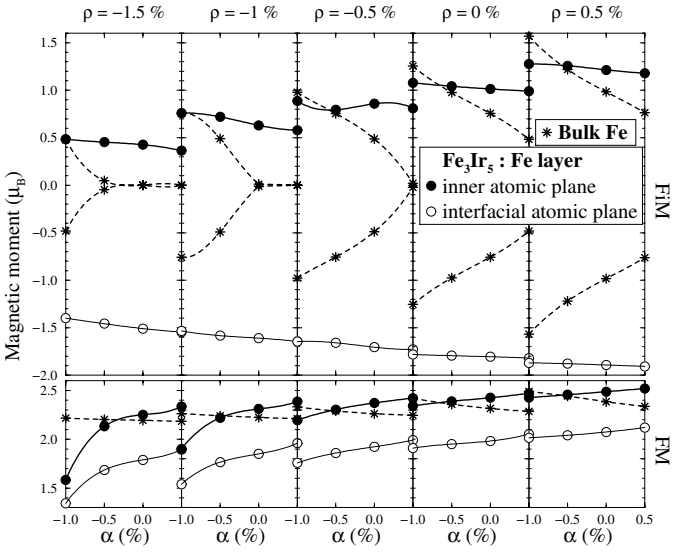

Fig. 5. Magnetic moments values on all non-equivalent Fe sites in the Fe_3Ir_5 superlattices for the ferromagnetic (FM) (lower graphs) and the ferrimagnetic (FiM) (upper graphs) configurations of the Fe layers for all (α, ρ) values of grid displayed in Table 1. The magnetic moments values are also given for the FM and the AFM bulk BCT orders (star symbols) for comparison with respectively the FM and FiM ones.

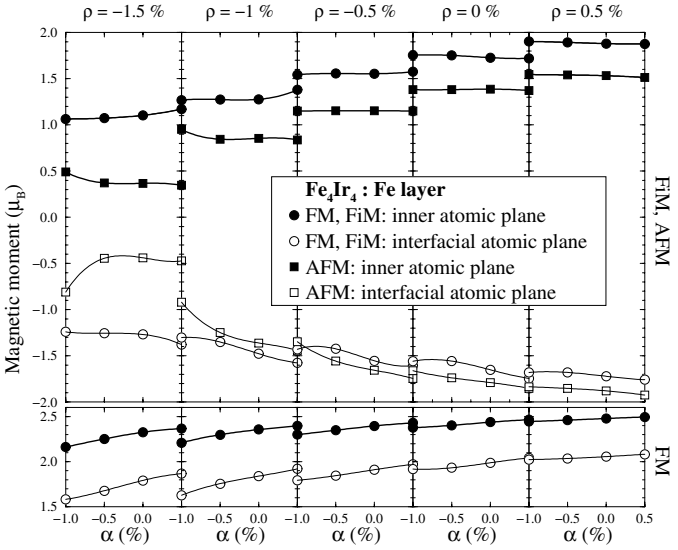

Fig. 6. Magnetic moments values on all non-equivalent Fe sites in the Fe_4Ir_4 superlattices for the ferromagnetic (FM) (lower graphs) and the ferrimagnetic (FiM) and antiferromagnetic (AFM) (upper graphs) configurations of the Fe layers for all (α, ρ) values of grid displayed in Table 1.

BCT. For example, the interfacial magnetic moment can reach more than -1.7 μ_B whereas the corresponding bulk BCT structure is non magnetic. This confirms the high level of stability of anti-aligned magnetic orders in these thin Fe layers in contact with Ir layers. For larger Fe thickness (Figs. 6 and 7), these trends remain valid: the main

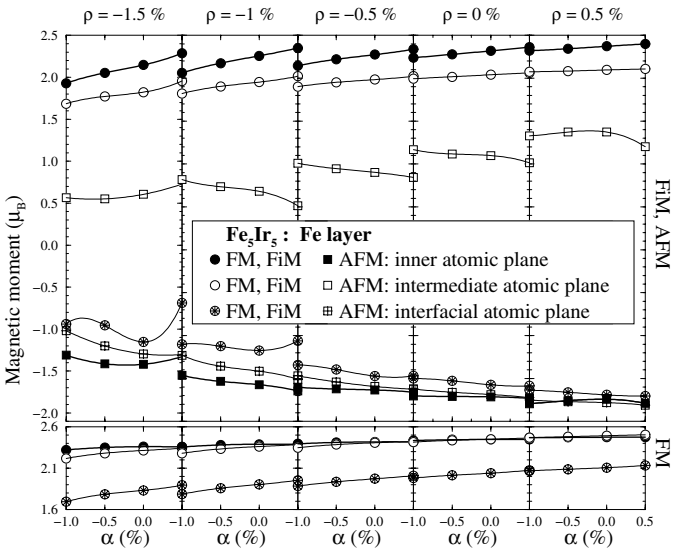

Fig. 7. Magnetic moments values on all non-equivalent Fe sites in the Fe_5Ir_5 superlattices for the ferromagnetic (FM) (lower graphs) and the ferrimagnetic (FiM) and antiferromagnetic (AFM) (upper graphs) configurations of the Fe layers for all (α, ρ) values of grid displayed in Table 1.

emerging feature is a higher sensitivity of the interfacial Fe magnetic moment to α variations for small values of ρ.

It is a priori expected that the AFM order should be hard to stabilise in a large part of the (α, ρ) domain of variation considered in this section because it is unstable in the corresponding bulk BCT structure (see Tab. 2 and Fig. 5). Surprisingly, even if from an energetically point of view it is always less stable than the FiM order (see next paragraph), an AFM solution is obtained for all values of (α, ρ) as it can be seen in Figures 6 and 7. The local magnetic moments are always smaller in magnitude to the ones obtained for the FiM case but behave completely different than in the bulk BCT case. This is a second confirmation of the stabilisation of magnetic anti-alignments in these thin Fe layers over all their thickness.

We conclude from these data that the thin Fe layers in the Fe/Ir superlattices exhibit a magnetic behaviour significantly different from bulk BCT with an emerging tendency to magnetic anti-alignments.

3.6 Magnetic phase (α, ρ) diagrams

In this paragraph we consider the relative energy stability of the various magnetic orders considered and discussed more in details in the previous paragraph. First, we found that the AFM order is always less stable than the FiM one and will not be included in our discussion. We have determined the polynomial functions $P_{\mathrm{MS}}(\alpha, \rho)$ interpolating the calculated total energies values for the FM, FiM and NM situations and derived the most stable one for all (α, ρ) values. The resulting phase diagrams obtained for the 3 Fe layers thickness considered in this section are reported in Figure 8 by plotting the limit of the stability domain of each situation.

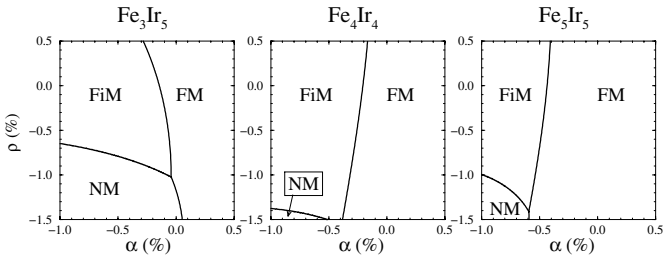

Fig. 8. Magnetic phases diagram for Fe_3Ir_5, Fe_4Ir_4 and Fe_5Ir_5 superlattices. The lines delimit the domain of stability in the (α, ρ) two dimensional space of each magnetic configuration.

The 3 diagrams present the same structure: the FM stability domain dominates the right part, the left part is split into the NM stability domain at the bottom and the FiM stability domain at the top. This is completely different from what has been obtained for bulk BCT where the FM magnetic state dominates the entire phase diagram in the studied range of (α, ρ) values. If we consider Table 2 and the discussion of paragraph *a*, we can deduce the following trends for the bulk BCT Fe: (i) the FM order is stabilised by increasing α, (ii) the NM-FM difference is the lowest for $\rho = \alpha$ and more especially for small ρ values corresponding to a compression of the volume of the cell which is well known as reducing the strength of the magnetism, (iii) the AFM order is stabilised by increasing the tetragonal character of the cell (given by $\Delta E_{\mathrm{AFM-FM}}$ for large c/a ratio values). These trends remain valid for the superlattices, showing that they are dominated by the bulk BCT Fe behaviour and that the main new feature revealed by the phases diagrams of the superlattices is to move the crossing lines between the different orders in the range of tetragonal distortions – around the experimental structure – we consider here. Moreover, the triple point is included (or nearly included) in our phase's diagrams. This shows that the relation between magnetism and structure is richer in Fe thin layers in Fe/Ir superlattices than in bulk BCT.

When the Fe thickness increases (from 3 to 5 monolayers), the FM domain limit is shifted to smaller α values as expected but, even for Fe_5Ir_5 superlattices, the bulk BCT behaviour is far from being recovered. Surprisingly, the FiM-FM separation line correspond approximately to a vertical line: this shows that the in plane parameter controls the competition between the FM and the FiM orders and the atomic volume plays a minor role in the range of values considered in this work (it controls mostly the separation line between FiM and NM orders).

The experimental structure for thin Fe layers corresponds nearly to the point $\alpha = 0$ and $\rho = 0$ in the diagrams. For Fe_3Ir_5 and Fe_4Ir_4 superlattices, this point is close to the FiM-FM separation line whereas it is clearly located in the FM domain for Fe_5Ir_5 superlattices. This result can explain why small magnetisation have been obtained experimentally for thin Fe layers [8] but cannot explain the conclusion of Mössbauer measurements showing that the interfacial Fe atoms carry nearly no magnetic moment [12].

4 Interlayer magnetic couplings and Ir induced polarisation

Calculating the interlayer magnetic couplings is a priori more easier than the energies discussed in Section 3. We have to determine the total energy difference $\Delta E_{\mathrm{F-AF}}$ between the ferromagnetic (F) and the antiferromagnetic (AF) interlayer magnetic arrangements: F corresponds to aligned magnetisation for successive Fe layers whereas AF corresponds to anti-aligned ones. However, we have to do these calculations for $\mathrm{Fe}_m\mathrm{Ir}_n$ superlattices with increasing Ir thickness in the magnetic cell (the AF one) containing $2 \times (m+n)$ non equivalent atoms. Moreover, because the interlayer couplings diminish when n increases, more K-points are needed to obtain accurate total energies values. Consequently, for large Ir thickness the computation time becomes very large and supercomputing facilities are needed.

In the experiments, the interlayer couplings have been studied for large Fe thickness where the Fe layer structure is nearly relaxed. In agreement with experiments [7], we choose the in plane parameter $a = 5.293$ u.a. $=$ 2.8 Å (giving $\alpha \approx 5.6\%$), the c/a ratio for the Fe layers equal to 1.043 (giving $\rho \approx -1.1\%$) and the atomic volume radius for the Ir atoms equal to 2.8742 a.u. The Fe layers are then nearly in a BCC structure and the Ir layers nearly in a FCC one. Finally, we choose to study $\mathrm{Fe_5Ir}_n$ superlattices with $n = 1$ to 11 monolayers for having a significantly thick Fe layer and a not to large elemental cell.

When calculating directly the magnetic moments profiles and the interlayer magnetic couplings using band structure methods, we have to take into account the discrete character of the spacer [21]. This introduces an aliasing effect on the period of the oscillating polarisation and interlayer coupling. For example, if we assume that the induced polarisation $\delta\mu(z)$ oscillates with a period of λ, the effective period λ_{eff} is then equal to:

$$\lambda_{\mathit{eff}} = \frac{1}{\left|\frac{1}{\lambda} - \frac{\nu}{d}\right|} \qquad (1)$$

where ν is a non-negative integer usually equal to one and d the spacing between monolayers. It is interesting to remark that λ_{eff} becomes larger when λ becomes closer to d. The effective period is the one deduced from the calculation.

Figure 9 shows the magnetic moments profiles in the Ir spacer layer for F and AF orders for all considered Ir thickness. The Ir spacer is much more polarised for this structure than for the ones considered in the previous section: the interfacial magnetic moment is nearly equal to 0.15 μ_B whereas previously it was always smaller than 0.05 μ_B. This is ascribed to a magnetic susceptibility enhancement resulting from the increase of the Ir atomic volume by 7%. The comparison of the profiles obtained for F and AF situations, shows that they become rapidly similar at the interface with Fe when n is increased: for large n values, they differ only on the inner Ir sites related to the node in the magnetic polarisation required by the AF configuration. Indeed, the magnetic symmetry of the superlattice and the parity of the Ir thickness induce different constraints on the magnetic moments on the inner sites: (i) for a F (respectively AF) interlayer arrangement, the two inner magnetic moments have to be equal (respectively opposite) when n is even and (ii) for an AF interlayer arrangement, the magnetic moment on the central site has to be exactly equal to zero when n is odd. This plays an essential role on the polarisation for the smallest thickness as can be seen in Figure 9 for $n = 1$, 2 and 3. The interfacial Ir moment is a priori strongly polarised by hybridisation with the Fe layer but large values are obtained for $n = 1$ and 3 when the interlayer arrangement is F and for $n = 2$ when it is AF. This has to be correlated to the beginning of the oscillation of the polarisation that favours a negative magnetic moment on the second Ir layer. When such a negative magnetic moment is allowed, the moments are larger. For larger Ir layers, this interaction between the oscillation and the magnetic symmetry continues to act only on the inner magnetic moments. Consequently, the most stable interlayer arrangement, i.e. the interlayer magnetic coupling, should reflect the compatibility between the oscillating polarisation and the magnetic symmetry of the magnetic moment profiles in the spacer. Because we consider only small spacer thickness, it is not possible to obtain very accurately the period of the oscillation. However, if we use the polarisation obtained for $n = 10$ and 11, and by fitting with [22]:

$$M(n) = M_0 F(n) \quad \text{with} \quad F(n) = \frac{\cos\left(\frac{2\pi}{\lambda_{\mathit{eff}}} nd + \varphi\right)}{n^{\eta}} \qquad (2)$$

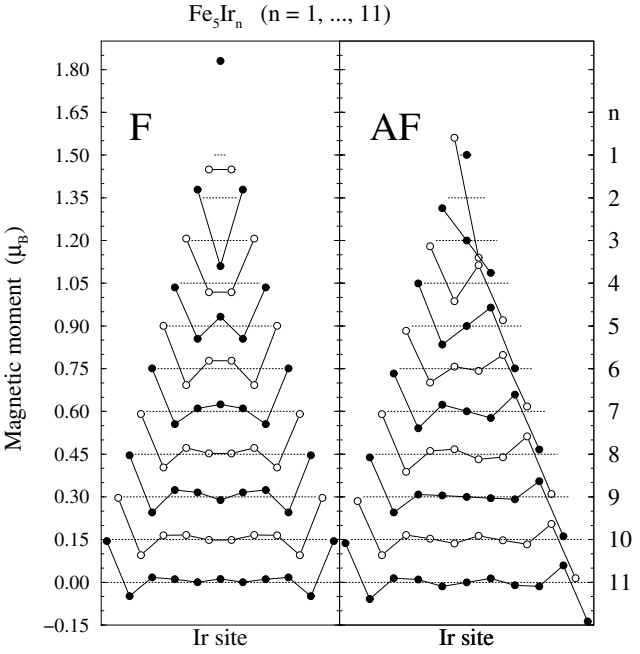

Fig. 9. Magnetic moments profiles in the Ir spacer layer for $\mathrm{Fe_5Ir}_n$ superlattices ($n = 1$ to 11 monolayers) for F and AF interlayer magnetic arrangements. The dashed lines give the zero for each profile; the profiles being shifted by 0.15 μ_B from one thickness to the other.

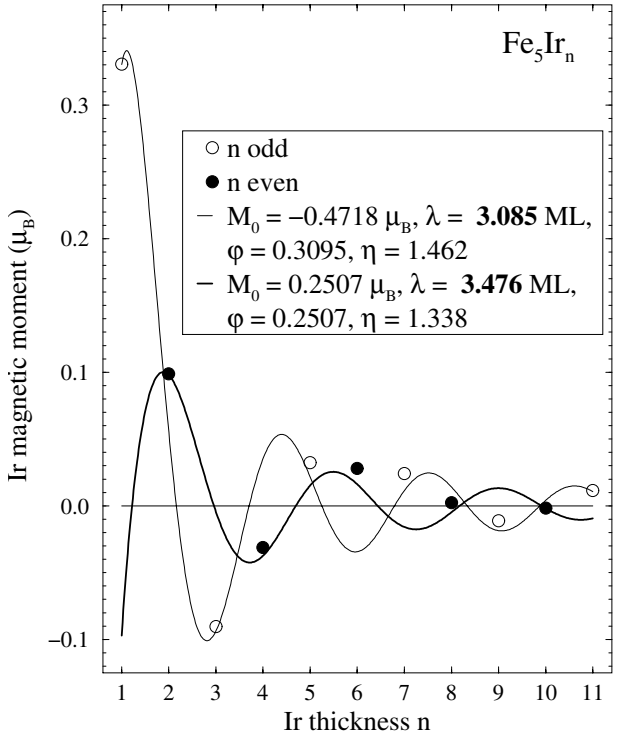

Fig. 10. Magnetic moments on the central sites of the Ir spacer layer for Fe_5Ir_n superlattices (n = 1 to 11 monolayers) for the F interlayer magnetic arrangement. The values for different parity of n are treated separately and the curves in solid lines correspond to the fits.

Table 4. Fits parameters of the curves displayed in Figure 10 using equation (2).

	$M_0\mu_B$)	$\lambda_{eff}/d(\lambda/d)$	φ	η
n odd	−0.472	3.085 (1.480)	0.310	1.462
n even	−0.251	3.476 (1.404)	−0.635	1.338

we obtain $\lambda_{eff} \cong 3.02d$ and $2.63d$ for the F arrangements and $\lambda_{eff} \cong 2.57d$ and $2.82d$ for the AF arrangements corresponding respectively to $\lambda \cong 1.50d$, $1.61d$, $1.64d$ and $1.55d$.

Figure 10 presents the magnetic moment on the inner sites as a function of the Ir spacer thickness n for the F interlayer arrangement. When we analyse the curves separately for the two parity of n, they can be easily fitted using (2) and the parameters of the fits are given in Table 4.

The interlayer coupling given by the total energy difference ΔE_{F-AF} and displayed in Figure 11 oscillates as a function of n with a period $\lambda_{eff} \cong 3.2d$ corresponding to $\lambda \cong 1.45d$ but only a poor fit using an expression similar to (2) is obtained. This period corresponds approximately to the ones given in Table 4 and to the ones deduced directly from the polarisation. Depending on the shape of the Fermi surface, the induced polarisation and the interlayer couplings can result from a superposition of contributions with different periods [21] but the phases and the strengths of each contribution is different between the polarisation and the couplings. In the present system, where the Fermi surface of bulk Ir is known as being complex, this study shows that only one period is required. This work shows also explicitely the connection between the period of the induced polarisation and of the interlayer couplings that can be analysed in terms of the constraint applied on the magnetic moment profiles by the magnetic symmetry in the spacer.

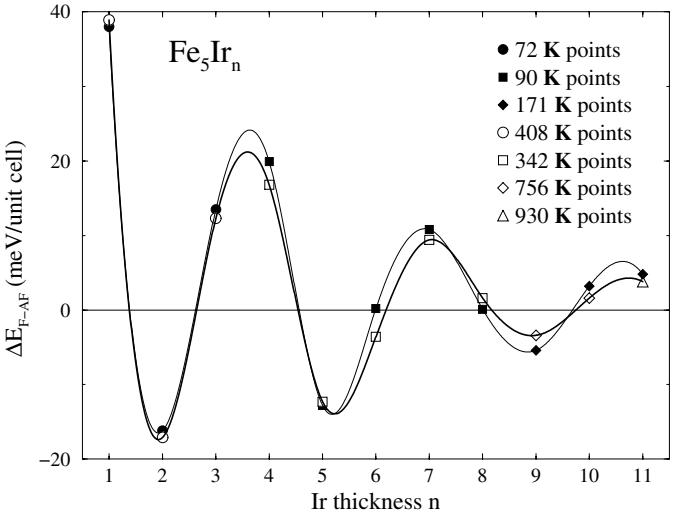

Fig. 11. Interlayer magnetic couplings $\Delta E_{\mathrm{F-AF}}$ for Fe_5Ir_n superlattices as a function of n. For each value of n, the coupling obtained with the 2 largest number of K-points used are given. The curves are only guide for the eyes.

5 Conclusion

This work has shown that it is extremely difficult to obtain, by band structure calculations, interfacial Fe atoms carrying no magnetic moment in Fe/Ir superlattices even by considering magnetic configurations with anti-aligned Fe magnetic moments. This result is a priori in contradiction with the one obtained for thin strained BCC [23] or FCC [24] Fe films on Ir(001) where vanishing interfacial Fe moments have been obtained. However, it is more the compression of the atomic volume which is at the origin of this vanishing than the hybridisation with Ir: the 4 Fe atomic layers from the interface carry small magnetic layers and only the surface magnetic moment remains magnetically alive due to the coordination reduction. Consequently, this calculation cannot also explain the observed behaviour.

To summarize, we have shown that (i) the magnetism in these thin Fe layers is reinforced as compared to bulk BCT, (ii) for FM and FiM magnetic configurations of the Fe layers, the interfacial Fe moment is robust relative to deformations of the BCT cell, and (iii) a non magnetic solution can be stabilized only for Fe_3Ir_5 superlattices when the BCT cell is compressed. These results disagree a priori with the experimental ones where the interfacial Fe atoms are found magnetically dead [12]. At this stage of the study it is not clear if the vanishing of the Fe interfacial moments

cannot be accounted by electronic structure considerations or if the interface is more complex than the flat one assumed here. Future work will concentrate on this second aspect by introducing interfacial alloying.

References

1. S. Andrieu et al., J. Magn. Magn. Mater. **121**, 30 (1993)
2. S. Andrieu et al., J. Magn. Magn. Mater. **126**, 349 (1993)
3. S. Andrieu et al., Europhys. Lett. **26**, 189 (1994)
4. A. Traverse et al., Surface Science **319**, 131 (1994)
5. S. Andrieu, M. Hennion, M. Piecuch, Mat. Res. Soc. Symp. Proc. **313**, 135 (1993)
6. S. Andrieu et al., J. Appl. Phys. **77**, 1308 (1995)
7. S. Andrieu et al., Phys. Rev. B **52**, 9938 (1995)
8. S. Andrieu et al., J. Magn. Magn. Mater. **148**, 6 (1995)
9. P. Bauer, S. Andrieu, L. Piecuch, Il Nuovo Cimento D **18**, 299 (1996)
10. E. Snoeck et al., J. Crystal Growth **167**, 143 (1996)
11. H. Renevier et al., Phys. Rev. Lett. **78**, 2775 (1997)
12. Ph. Bauer et al., J. Magn. Magn. Mater. **165**, 220 (1997)
13. M. Henkel et al., Phys. Rev. Lett. **80**, 4783 (1998)
14. S. Andrieu et al., Phys. Rev. Lett. **86**, 3883 (2001)
15. A.R. Williams, J. Küber, C.D. Gelatt, Jr., Phys. Rev. B **19**, 6094 (1979)
16. R. Coehoorn, Phys. Rev. B **44**, 9331 (1991)
17. F. Herman, J. Sticht, M. van Schilfgaarde, Mat. Res. Soc. Symp. Proc. **231**, 195 (1992)
18. D. Stoeffler et al., Phys. Rev. B **49**, 299 (1994); E.E. Fullerton et al. Phys. Rev. B **51**, 6364 (1995)
19. S. Zoll et al., Europhys. Lett. **39**, 323 (1997)
20. V.L. Moruzzi et al., Phys. Rev. B **34**, 1784 (1986)
21. P. Bruno, C. Chappert, Phys. Rev. B **46**, 261 (1992)
22. Equation (2) is a generalization of standard expressions used in Friedel-like oscillations, in induced polarization and interlayer couplings (and even in RKKY models) which gives the spatial charge variation as a function of the distance $d = n.c/2$ to the magnetic perturbation (an impurity or a layer). The expression used makes no assumption on the decay (η exponent which is usually equal to 3 for an impurity, equal to 2 for a layer and can even be smaller than 2 in case of nested Fermi surface [21]), on the spatial period λ_{eff} (which is related to the inverse of the Fermi vector [21]) and on the phase (φ which is related to the perturbating potential or to the matching of the wave functions at the Fe/Ir interface [21])
23. K. Louzazna, A. Haroun, Solid State Comm. **112**, 649 (1999)
24. K. Louzazna, A. Haroun, Thin Solid Films **374**, 114 (2000)